



A string-driven rotor for efficient energy harvesting from ultra-low frequency excitations

Cite as: Appl. Phys. Lett. **115**, 203903 (2019); <https://doi.org/10.1063/1.5128397>

Submitted: 18 September 2019 . Accepted: 04 November 2019 . Published Online: 13 November 2019

Kangqi Fan , Yiwei Zhang, Shiju E, Lihua Tang , and Hengheng Qu



View Online



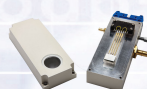
Export Citation



CrossMark



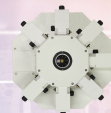
**THE WORLD'S RESOURCE FOR
VARIABLE TEMPERATURE
SOLID STATE CHARACTERIZATION**



OPTICAL STUDIES SYSTEMS



SEEBECK STUDIES SYSTEMS



MICROPROBE STATIONS



HALL EFFECT STUDY SYSTEMS AND MAGNETS

WWW.MMR-TECH.COM

A string-driven rotor for efficient energy harvesting from ultra-low frequency excitations

Cite as: Appl. Phys. Lett. **115**, 203903 (2019); doi: [10.1063/1.5128397](https://doi.org/10.1063/1.5128397)

Submitted: 18 September 2019 · Accepted: 4 November 2019 ·

Published Online: 13 November 2019



View Online



Export Citation



CrossMark

Kangqi Fan,^{1,a)}  Yiwei Zhang,¹ Shiju E,² Lihua Tang,^{3,a)}  and Hengheng Qu¹

AFFILIATIONS

¹School of Mechano-Electronic Engineering, Xidian University, Xi'an 710071, China

²College of Engineering, Zhejiang Normal University, Jinhua 321004, China

³Department of Mechanical Engineering, University of Auckland, Auckland 1010, New Zealand

^{a)}Authors to whom correspondence should be addressed: kangqifan@gmail.com and l.tang@auckland.ac.nz

ABSTRACT

This Letter reports a string-driven rotor for constructing ultralow frequency energy harvesters. Consisting of a disk-shaped rotor with a shaft, an elastic string, and an inelastic string, the proposed rotor structure can convert ultralow frequency vibrations or linear reciprocating motions to high-speed rotation of the rotor without any sophisticated transmission mechanism. On the basis of the string-driven rotor, an electromagnetic energy harvester is designed, and the corresponding theoretical model is established. Both simulation and experiments demonstrate the high output performance of the harvester under a periodic excitation with an amplitude of 5 mm and at a frequency lower than 5 Hz. The harvester also generates 6.5 mW power when driven by hand at a frequency of approximately 4 Hz. This study exhibits the exciting potential of the string-driven rotor for boosting the efficiency of harvesting energy from pervasive ultralow frequency excitations.

Published under license by AIP Publishing. <https://doi.org/10.1063/1.5128397>

Harvesting ambient kinetic energy for power generation has been deemed as a promising approach for achieving self-powered electronics due to its ubiquitous nature.^{1,2} Kinetic energy, which comes in different forms as diverse as vibration, rotation, and swing motion, can be converted into electricity via a number of transduction mechanisms, such as electromagnetic induction,^{3,4} piezoelectric effects,^{5,6} electrostatic induction,^{7,8} and triboelectrification.⁹ To achieve a simple configuration and easy integration with small-scale electronics, these transduction mechanisms have been widely used with cantilevered structures to construct various vibratory energy harvesters (VEHs) that can directly generate electricity from ambient vibrations. For other forms of mechanical motion, additional transmission mechanisms are usually required to actuate the VEHs to work.^{10,11} Since the linear VEHs normally behave poorly under off-resonant conditions and thus suffer from a narrow bandwidth, great effort has been made to expand the working bandwidth.^{12,13} The outcomes of these efforts are several broadband harvesting strategies, including tuning the resonance,¹⁴ employing multimodal designs,¹⁵ and invoking nonlinear dynamic responses (softening response,¹³ hardening response,¹⁶ nonlinear energy sink,¹⁷ and internal resonance¹⁸). Due to size or dynamic constraints,^{19,20} although these broadband VEHs can achieve improved performance compared with their linear counterparts, they still fail to perform well under omnipresent ultralow frequency (<5 Hz) excitations (such as wave heave motions, human body motions, and bridge deformations due to the action of traveling vehicles).

One possible way to maintain the functionality of VEHs under ultralow frequency excitations is exploiting the frequency upconversion (FUC) technology, which employs one subsystem to sense ultralow frequency excitations and then triggers another subsystem with high resonant frequency to generate electricity through magnetic force or mechanical impact/plucking.^{21–23} Disadvantages of the FUC technology may involve enhanced structural complexity and extra energy dissipation for transmitting motion between different subsystems. Another way to realize ultralow frequency VEHs is replacing the cantilever structures with repulsively magnetic force that suspends a magnetic mass within a cylindrical tube surrounded with pickup coils.^{24,25} However, electric outputs of the cylindrical VEHs are comparatively low owing to the slow change rate of the magnetic flux across the pickup coils under ultralow frequency excitations. In recent years, researchers have explored rotational energy harvesters (REHs) with various rotors to capture energy from ultralow frequency excitations.^{3,26} The conventional rotor structure has been investigated widely and developed well in the macro scale,^{27,28} but their efficiency drops quickly after being miniaturized.²⁹ Moreover, since the naturally available excitations (such as mechanical vibrations, linear reciprocating motions, swing motions) cannot trigger the rotation of the conventional rotor, additional eccentric mass has to be attached to the rotor, which enables the (eccentric) rotor to do swing motion with respect to the stator under ambient excitations.^{4,30} Due to the cause akin to that

for cylindrical VEHs, the swing-motion based REHs can only provide low power outputs (<0.1 mW) under ultralow frequency excitations.

This Letter reports a string-driven rotor for constructing REHs with intent to achieve efficient conversion of ambient ultralow frequency mechanical energy into electric energy. Different from the aforementioned eccentric rotor whose operation relies on the torque produced by the eccentric mass, the string-driven rotor utilizes an elastic string and an inelastic string to convert ultralow frequency excitations to high-speed rotation of the rotor. High electric outputs can then be expected from the REHs realized with the string-driven rotor. We demonstrate the working principle of the string-driven rotor as well as its promising application in energy harvesting through an electromagnetic energy harvester.

The schematic diagram of the string-driven rotor is illustrated in Fig. 1(a), which consists of a disk-shaped rotor supported by a shaft with two grooves, an elastic string and an inelastic string. One end of the elastic string is fixed to the device enclosure, and the other end is tied to the shaft at one of the two grooves. The inelastic string is attached to the other groove of the shaft, whereas the other end of the inelastic string is utilized to receive external excitations. Initially, the elastic string wraps around the shaft clockwise, whereas the inelastic string encircles the shaft in the opposite direction, as shown in the inset of Fig. 1(a). When an upward excitation pulls the inelastic string, a torque acting on the shaft is produced via the inelastic string, which drives the shaft to rotate anticlockwise and then reduces the number of laps that the inelastic string wraps around the shaft. In the meantime, the rotation of the shaft increases the number of laps of the elastic string surrounding the shaft. Since the distance between the shaft and the fixed point of the elastic string remains constant, the tension in the elastic string rises with the anticlockwise rotation of the shaft. After the external excitation is reversed, the tension in the elastic string drives the shaft to rotate clockwise, which reduces the number of laps of the elastic string wrapping around the shaft while it increases that of the inelastic string. This describes a full cycle of the rotation of the shaft, and this process will continue under a periodic excitation. Considering that the rotor rotates with the shaft, electricity can be generated based on the exploitation of the relative motion between the rotor and a stator through various transduction mechanisms.

Compared with the conventional rotor, the string-driven rotor can convert ambient ultralow frequency vibrations or linear reciprocating motions to rotation motion without additional complicated transmission mechanisms, permitting the realization of REHs with a simple structure. The string-driven rotor differentiates itself from the string-suspended and driven rotor³¹ in two major aspects: (1) the

former is supported by a shaft whereas the latter is suspended from a lid through a string without using a shaft; (2) the rotation of the former depends on the potential energy stored in the stretched elastic string while the rotation of the latter is the result of the interconversion between the potential energy stored in the twisted strings and the kinetic energy of the rotating rotor. In addition, the string-driven rotor differs from the eccentric rotor in that it does large-angle and high-speed rotation instead of swing motion (small-angle and low-speed rotation) under ultralow frequency excitations. As a result, high electric outputs can be expected from a REH designed with the string-driven rotor. To test this hypothesis, we devise an electromagnetic REH on the basis of the proposed rotor, as shown in Fig. 1(b). To generate electricity through electromagnetic induction, six magnets (Nd-Fe-B) are radially arrayed within the rotor and six sets of pickup coils each with 100 turns are attached to the tube (device enclosure) in a similar way. The six coils are connected in series for providing a high voltage level. To ensure the smooth rotation, a bearing, which is embedded within the lid of the tube, is employed to support the rotor via the shaft. The elastic string (thermoplastic polyurethanes) threads through hole 1 and is fixed to the tube, and the inelastic polyester string is connected to an external excitation source through hole 2 of the tube. The rotor, tube, and lid are all fabricated from UV Curable Resin using 3D printing technology, and the shaft is made of nylon plastic. The shaft has a size of 22 mm in length and $\Phi 8$ mm in diameter, but a reduced diameter of 4 mm at the grooves. The magnets each with a dimension of 6 mm \times 6 mm \times 3 mm are embedded within the rotor of $\Phi 30$ mm \times 6 mm. The harvester has a diameter of 38 mm and a length of 27.5 mm, yielding a total weight of 30 g.

When the inelastic string of the REH is subjected to an external excitation, the rotor will be driven to rotate by the tensile force F_2 in the inelastic string and the tensile force F_1 in the elastic string. The dynamic behavior of the system can be described as

$$\begin{cases} J\ddot{\theta} + C_m\dot{\theta} + \beta Ir_R = (F_2 - F_1)r_0 \\ L\dot{I} + (R_C + R_L)I = \beta r_R\dot{\theta}, \end{cases} \quad (1)$$

where J is the moment of inertia of the rotor and shaft, C_m the mechanical damping coefficient, β the electromechanical coupling coefficient, r_R the radius of the rotor, r_0 the radius of the shaft at the grooves, θ the rotation angle, R_L the electric load, and I the induced current; L and R_C denote the inductance and resistance of the coil, respectively.

Seeing that the normally utilized vibration exciter cannot produce ultralow frequency excitations, a crank-slider mechanism is devised to actuate the REH by attaching the inelastic string to the slider, as shown in Fig. 2(a). With the excitation from the crank-slider mechanism, the quantitative characterization of the REH can be made. The crank-slider mechanism is driven by a stepper motor with adjustable rotation speed. In the experiment, the motion amplitude and frequency of the slider are varied by changing the length of the crank and the rotation speed of the stepper motor, respectively. For a crank with length of l_1 , the displacement of the slider can be expressed as

$$z_s = l_1 \cos(\omega t) + \sqrt{l_2^2 - l_1^2 \sin^2(\omega t)} - l_2, \quad (2)$$

where l_2 is the length of the connecting rod and ω is the angular frequency of the stepper motor. When actuated by the slider through the inelastic string, the rotor rotates with the angular displacement described as $\theta = z_s/r_0$.

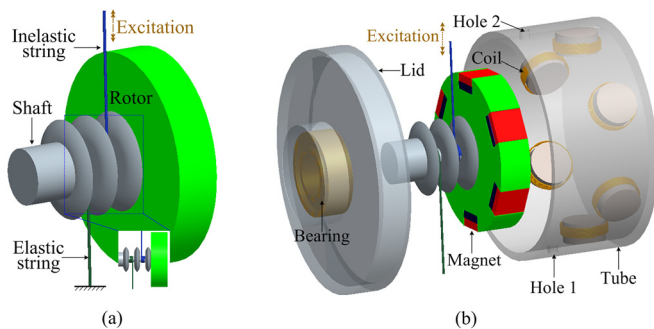


FIG. 1. (a) String-driven rotor; (b) electromagnetic REH with the string-driven rotor.

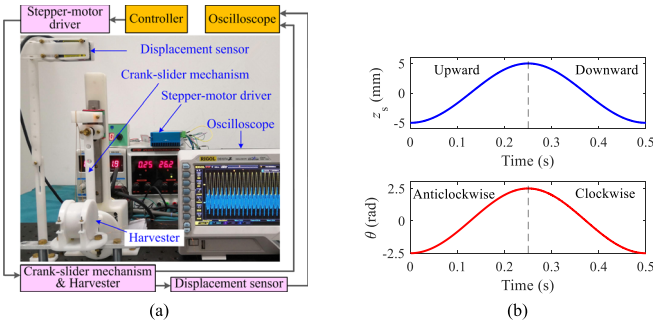


FIG. 2. (a) Electromagnetic harvester prototype with the experimental setup; (b) displacement of the slider and rotation angle of the rotor.

The tensile force in the elastic string when stretched can be calculated by the Mooney-Rivlin model³², i.e.,

$$F_1 = \frac{\pi d_s^2}{4l} \left[2C_1 \left(\lambda - \frac{1}{\lambda} \right) + 2C_2 \left(\lambda - \frac{1}{\lambda^3} \right) + 6C_3 \left(\lambda^2 - \lambda - 1 + \frac{1}{\lambda^2} + \frac{1}{\lambda^3} + \frac{1}{\lambda^4} \right) \right], \quad (3)$$

where d_s is the diameter of the elastic string without tension; $\lambda = (x_0 + \Delta x)/x_0$ with x_0 and Δx representing the original length and tensile elongation of the elastic string, respectively; C_1 , C_2 , and C_3 are model parameters that can be determined by fitting to experimental data.

With an initial tensile elongation of X_0 , the total elongation of the elastic string during the operation is

$$\Delta x = X_0 + z_s + l_1. \quad (4)$$

For the elastic string with different diameters, the original length remains constant ($x_0 = 21.5$ mm) and the parameters of the Mooney-Rivlin model are given in Table I.

For $l_1 = 5$ mm, $l_2 = 90$ mm, $\omega = 4\pi$ rad/s, and $r_0 = 2$ mm, the displacement of the slider and the rotation angle of the rotor are illustrated in Fig. 2(b). When the slider moves upward, the rotor is driven to rotate anticlockwise via the inelastic string. The clockwise rotation of the rotor is started by the stretched elastic string during the downward motion of the slider.

The experimental study is carried out using an inelastic string with a constant diameter of 0.6 mm, whereas the diameter of the elastic string varies from 0.4 mm to 0.8 mm. For each test, the inelastic string is tied to the slider when the latter is at the lowest position without stretching the elastic string (i.e., $X_0 = 0$), which results in an excitation amplitude of $l_1 = 5$ mm. The position of the slider is acquired by a laser sensor (HL-C203BE) and the electric outputs of the REH are measured using an oscilloscope (Rigol DS1074). When the REH is directly driven by a

TABLE I. Coefficients of the Mooney-Rivlin model.

D_s	C_1	C_2	C_3
0.4 mm	-3.84×10^7	3.27×10^7	2.06×10^7
0.6 mm	-4.01×10^6	2.29×10^5	1.22×10^6
0.8 mm	3.15×10^6	-4.08×10^6	9.52×10^6

TABLE II. System parameters.

Parameters	Value
J (g·mm ²)	1010
C_m (N·m·s·rad ⁻¹)	4×10^{-5}
β (Wb·m ⁻¹)	0.9
L (H)	0.083
R_C (Ω)	30
r_R (mm)	15

stepper motor with a constant rotation speed of 120 rpm (round per minute), the electromechanical coupling coefficient can be estimated as $\beta = V_{OC}/r_R\theta$, where V_{OC} is the root mean square (RMS) value of the open-circuit voltage. The mechanical damping coefficient C_m is obtained by fitting the theoretical predictions to the experimental measurements as well as possible under the same conditions.^{33,34} The system parameters used for theoretical simulations are given in Table II.

Figure 3 pictures the open-circuit voltage waveforms of the designed REH at two different frequencies in the case of $d_0 = 2r_0 = 4$ mm and $d_s = 0.6$ mm. When the excitation frequency is small (e.g., 3 Hz), the anticlockwise rotation of the rotor driven by the upward displacement of the slider can be fully recovered by the elastic string that pulls the rotor to rotate clockwise. As a result, the voltage magnitude is not sensitive to the rotation direction of the rotor. However, if the excitation frequency is large (e.g., 5 Hz), the elastic string can only partly revert the anticlockwise rotation of the rotor due to the reduced half cycle for the clockwise rotation of the rotor, which leads to smaller clockwise rotation speeds and

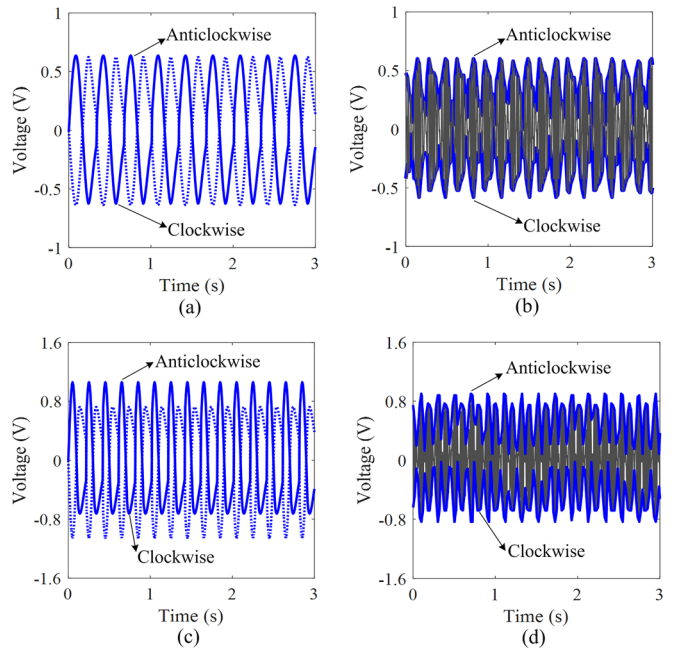


FIG. 3. Open-circuit voltage waveforms at various frequencies: (a) and (b) 3 Hz; (c) and (d) 5 Hz. (a) and (c) theoretical results; (b) and (d) experimental results with the envelope curve shown in blue.

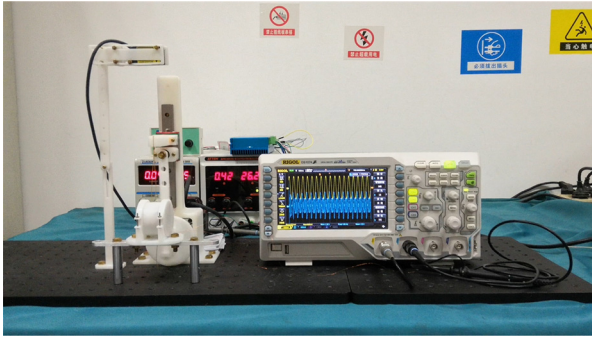


FIG. 4. Open-circuit voltage output of the REH at 5 Hz. Multimedia view: <https://doi.org/10.1063/1.5128397.1>

then lower voltage outputs during the clockwise rotation than those during the anticlockwise rotation of the rotor, as shown in Fig. 4 (Multimedia view). It should be mentioned that, for computational simplicity, an equivalent coupling coefficient β is generally utilized to describe the power generation in the simulations,^{4,24,34} which is assumed to produce negative outputs during the clockwise rotation and positive outputs during the anticlockwise rotation of the rotor. In fact, both positive and negative outputs are produced irrespective of the rotation direction. Therefore, the complete contour of the practical voltage output is the combination of the theoretical waveform and its mirrored waveform [dotted lines in Figs. 3(a) and 3(c)].

The theoretical and experimental power outputs as a function of the excitation frequency are shown in Fig. 5, in which the power is computed according to $P = V_{\text{RMS}}^2/R_L$, where V_{RMS} is the RMS voltage

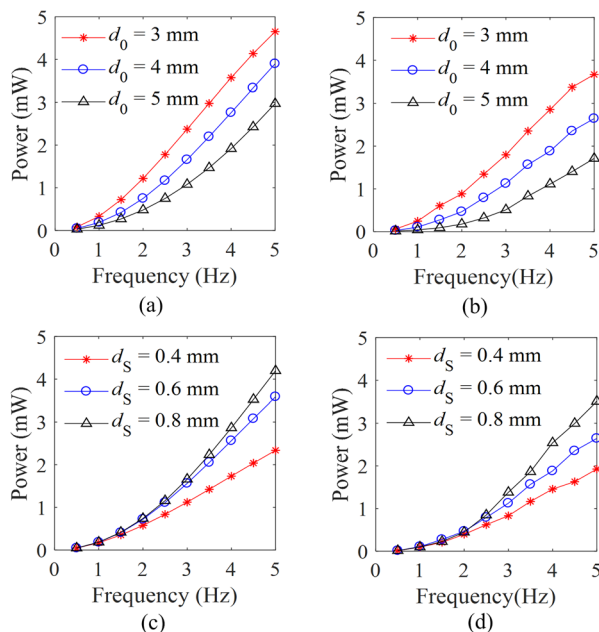


FIG. 5. (a) and (b) power outputs vs frequency at various values of d_0 ; (c) and (d) power outputs vs frequency at various values of d_s . (a) and (c) simulation; (b) and (d) experiment.

across the resistive load R_L (30Ω). Previous studies have shown that the power delivered to the resistive load equal to the coil resistance (30Ω) can be regarded as the optimal power due to the ignorable effect of the coil inductance under low-frequency (<1 kHz) operations.^{35,36} For the electromagnetic REH, the electric outputs rise with the increasing rotation speed of the rotor. Since the rotor rotates with an angular velocity ($2\dot{z}_s/d_0$) inversely proportional to the diameter ($d_0 = 2r_0$) of the shaft, increasing the value of d_0 will lead to the reduced angular velocity and then low power outputs, as shown in Figs. 5(a) and 5(b). For the diameter (d_s) of the elastic string, it has a positive relationship with the power outputs, as shown in Figs. 5(c) and 5(d). As the value of d_s increases, the tensile force in the elastic string goes up under the same value of elongation, which brings about an enlarged clockwise rotation speed of the rotor during the downward motion of the slider. Consequently, high power outputs can be achieved with a thick elastic string, particularly when the excitation frequency is relatively high. For a given value of d_0 or d_s , the designed REH can provide a power output that rises monotonously as the excitation frequency varies from 0.5 Hz to 5 Hz, which is attributed to the positive dependence of the rotation speed on the excitation frequency. The simulations predict the same trends of power outputs as the experiments although small differences can be observed. The discrepancy is probably owing to the constant damping coefficient used in the simulations, which may vary with the frequency in the experiment. In addition, winding the strings around the shaft and unwinding them due to the reciprocating rotation of the rotor will change the equivalent value of d_0 slightly, which is not taken into consideration in the simulations.

The REH is also driven by a human hand to examine its performance of harvesting energy from irregular human body motions, as shown in Fig. 6(a) (Multimedia view). Figure 6(b) plots the open-circuit voltage waveform when the human hand pulls the inelastic string of the REH with a frequency of around 4 Hz and amplitude of approximately 13 mm. Under this operation, the maximum voltage output can be as high as 1.35 V, and the power delivered to the matched load is 6.5 mW.

It should be noted that the primary objective of this study is to report a string-driven rotor and demonstrate its potential application in capturing energy from ultralow frequency excitations. Although little work has been done to optimize the string-driven rotor based REH, the produced power is still strikingly higher than that provided by previous REHs at similar frequencies. For comparison, the key characteristics of some typical REHs are shown in Table III, including the excitation frequency, REH's volume, output power, and the corresponding power density. Although there are a large number of parameters for characterizing the REHs, the parameters shown in Table III are generally adopted as they provide the fundamental information of the REHs, such as the working frequency, occupied volume, and the attainable power level.^{3,37} It is evident that the proposed REH can provide a remarkably high output power under ultralow frequency excitations. One exception of this observation is the nonresonant REH proposed by Liu *et al.*,³ which produces the highest power among the REHs in Table III. However, it is worth noting that the power of the nonresonant REH is acquired when it is actuated by shaking the hand with a much larger amplitude and high frequency of 8 Hz.

In summary, this Letter reports a string-driven rotor that can convert vibrations or linear reciprocating motions to high-speed rotation without any sophisticated transmission mechanism. Based on the string-driven rotor, an electromagnetic REH is designed and the

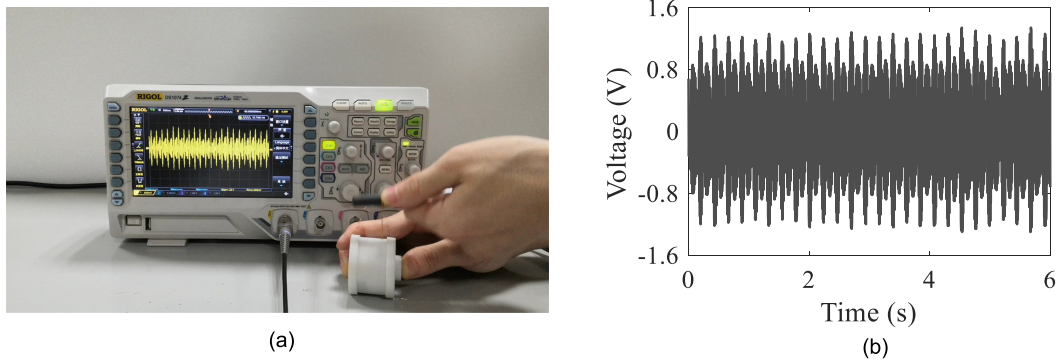


FIG. 6. (a) Driving the REH by hand and (b) open-circuit voltage waveform. Multimedia view: <https://doi.org/10.1063/1.5128397.2>

TABLE III. Performance comparison of typical REHs.

References	Excitation frequency (Hz)	Harvester volume (cm ³)	Output power (mW)	Power density (mW cm ⁻³)
Liu <i>et al.</i> ³	8	33.1	10.4	0.314
Halim <i>et al.</i> ⁴	1	8.5	0.06	0.007
Rantz <i>et al.</i> ³⁸	1.25	–	0.08	–
Smilek <i>et al.</i> ²⁶	3.45	50	1.40	0.028
This work	4	31.2	6.5	0.208

corresponding theoretical model is established. Both the experiment and simulation exhibit the high voltage and power outputs of the designed REH under ultralow frequency excitations. When the REH is excited by hand at around 4 Hz, it delivers up to 6.5 mW output power, which is substantially higher than that provided by previous REHs at similar frequencies. This study demonstrates the exciting potential of the string-driven rotor in boosting energy harvesting from environmental ultralow frequency excitations.

This research was supported by the National Natural Science Foundation of China (No. 51777147), the Natural Science Basic Research Plan in Shaanxi Province of China (No. 2018JM5030), and the Innovation Fund of Xidian University (No. 20109195867).

REFERENCES

- H. Liu, J. Zhong, C. Lee, S.-W. Lee, and L. Lin, *Appl. Phys. Rev.* **5**, 041306 (2018).
- G. Hu, J. Wang, Z. Su, G. Li, H. Peng, and K. C. S. Kwok, *Appl. Phys. Lett.* **115**, 073901 (2019).
- H. Liu, C. Hou, J. Lin, Y. Li, Q. Shi, T. Chen, L. Sun, and C. Lee, *Appl. Phys. Lett.* **113**, 203901 (2018).
- M. A. Halim, R. Rantz, Q. Zhang, L. Gu, K. Yang, and S. Roundy, *Appl. Energy* **217**, 66 (2018).
- H. Fu, Z. Sharif-Khodaei, and F. Aliabadi, *Appl. Phys. Lett.* **114**, 143901 (2019).
- S. C. Stanton, A. Erturk, B. P. Mann, and D. J. Inman, *J. Appl. Phys.* **108**, 074903 (2010).
- Y. Zhang, T. Wang, A. Luo, Y. Hu, X. Li, and F. Wang, *Appl. Energy* **212**, 362 (2018).
- K. Tao, J. Wu, L. Tang, L. Hu, S. W. Lye, and J. Miao, *J. Micromech. Microeng.* **27**, 044002 (2017).
- G. Zhu, J. Chen, T. Zhang, Q. Jing, and Z. L. Wang, *Nat. Commun.* **5**, 3426 (2014).
- B. Yang, Z. Yi, G. Tang, and J. Liu, *Appl. Phys. Lett.* **115**, 063901 (2019).
- S. Roundy and J. Tola, *Smart Mater. Struct.* **23**, 105004 (2014).
- S. Zhou, J. Cao, D. J. Inman, S. Liu, and W. Wang, *Appl. Phys. Lett.* **106**, 093901 (2015).
- K. Q. Fan, Q. X. Tan, Y. W. Zhang, S. H. Liu, M. L. Cai, and Y. M. Zhu, *Appl. Phys. Lett.* **112**, 123901 (2018).
- M. Lallart, S. R. Anton, and D. J. Inman, *J. Intell. Mater. Syst. Struct.* **21**, 897 (2010).
- A. Erturk, J. M. Renno, and D. J. Inman, *J. Intell. Mater. Syst. Struct.* **20**, 529 (2009).
- S. Zhou and L. Zuo, *Commun. Nonlinear Sci.* **61**, 271 (2018).
- D. Kremer and K. Liu, *J. Sound Vib.* **333**, 4859 (2014).
- L. Xiong, L. Tang, and B. R. Mace, *Appl. Phys. Lett.* **108**, 203901 (2016).
- F. Cottone, H. Vocca, and L. Gammaitoni, *Phys. Rev. Lett.* **102**, 080601 (2009).
- D. A. W. Barton, S. G. Burrow, and L. R. Clare, *J. Vib. Acoust.* **132**, 021009 (2010).
- Y. Kuang and M. Zhu, *Smart Mater. Struct.* **25**, 055013 (2016).
- H. Fu and E. M. Yeatman, *Mech. Syst. Signal Pr.* **125**, 229 (2018).
- K. Q. Fan, Z. H. Liu, H. Y. Liu, L. S. Wang, Y. M. Zhu, and B. Yu, *Appl. Phys. Lett.* **110**, 143902 (2017).
- B. P. Mann and N. D. Sims, *J. Sound Vib.* **319**, 515 (2009).
- B. P. Mann and B. A. Owens, *J. Sound Vib.* **329**, 1215 (2010).
- F. Smilek, Z. Hadas, J. Vetiska, and S. Beeby, *Mech. Syst. Signal Pr.* **125**, 215 (2019).
- S. Torabnia and A. Banazadeh, "Development of a Water Brake Dynamometer With Regard to the Modular Product Design Methodology," *Proc. ESDA 20232* (2014).
- S. Torabnia, M. Hemati, and S. Aghajani, *Mater. Sci. Forum.* **969**, 669 (2019).
- S. Priya, *J. Electroceram.* **19**, 167 (2007).
- P. Pillatsch, E. M. Yeatman, and A. S. Holmes, *Sens. Actuators A* **206**, 178 (2014).
- K. Fan, M. Cai, F. Wang, L. Tang, J. Liang, Y. Wu, H. Qu, and Q. Tan, *Energy Convers. Manage.* **198**, 111820 (2019).
- N. Kumar and V. V. Rao, *MIT Int. J. Mech. Sci.* **6**, 43 (2016).
- G. Sebald, H. Kuwano, D. Guyomar, and B. Ducharme, *Smart Mater. Struct.* **20**, 102001 (2011).
- W. Liu, C. Liu, B. Ren, Q. Zhu, G. Hu, and W. Yang, *Appl. Phys. Lett.* **109**, 043905 (2016).
- M. F. Daqaq, *J. Sound Vib.* **330**, 2554 (2011).
- T. O'Donnell, C. Saha, S. Beeby, and J. Tudor, *Microsyst. Technol.* **13**, 1637 (2007).
- K. Fan, Q. Tan, H. Liu, M. Cai, and H. Qu, *Smart Mater. Struct.* **28**, 07LT01 (2019).
- R. Rantz, M. A. Halim, T. Xue, Q. Zhang, L. Gu, K. Yang, and S. Roundy, *Smart Mater. Struct.* **27**, 044001 (2018).